Ionics (2023) 29:4275–4283
https://doi.org/10.1007/s11581-023-05140-6

RESEARCH

An anti-freezing and conductive glycerol-Mo-based organohydrogel electrolyte for flexible supercapacitor

Qing Xin[1] · Xiaojie Chu[1] · Guoqing Yang[1] · Shangqing Liang[1] · Jun Lin[1]

Received: 6 May 2023 / Revised: 27 June 2023 / Accepted: 22 July 2023 / Published online: 26 July 2023

Abstract
By partially substituting water molecules in polymer hydrogel electrolytes with organic solvents, the-low temperature tolerance of supercapacitors can be significantly improved. However, the low conductivity resulting from the organic solvents inevitably influences the energy storage behavior of the supercapacitor. To address this issue, a new strategy is employed by embedding glycerin (Gly)-Mo into both the electrolyte and electrode materials, resulting in a supercapacitor that exhibits outstanding conductivity and resistance to subzero temperatures. The introduction of Gly-Mo enhances the mechanical properties and conductivity of hydrogel under freezing conditions. The in situ growth of an electrode containing Gly-Mo lowers the interface resistance between the electrode and electrolyte. When the temperature decreases from room temperature to − 40 °C, the supercapacitor retains 63.36% of its specific capacitance. Furthermore, the flexible supercapacitor is capable of withstanding punching damage, maintaining a specific capacitance of 140.75 mF cm^{-2} at 1 mA cm^{-2} with 300 holes cm^{-2}. The supercapacitor also exhibits remarkable capacitance retention after being bent at a 90° angle for 400 cycles.

Keywords Gly-Mo · Organohydrogel · Subzero temperature tolerance · Flexible supercapacitor

Introduction

While the application of flexible supercapacitor as an energy storage device in wearable electronics is gaining acceptance, their performance at subzero temperatures caused by regional climate discrepancy or seasonal changes remains a problem [1]. A flexible supercapacitor typically adopts a polymer hydrogel electrolyte with a water-rich structure, which supplies good ion conductivity, mechanical properties or self-healing ability, etc. [2, 3]. At subfreezing temperatures, the supercapacitor's performance deteriorates due to limited ionic conductivity and loss of flexibility caused by the freezing of water in the hydrogel electrolyte [4, 5]. This problem severely limits the application of polymer hydrogel electrolyte-based supercapacitors in cold climates.

To address this issue, researchers are working to improve the anti-freezing property of the hydrogel electrolytes for actual application requirements. One simple solvent replacement strategy is put forward. By replacing a portion of water molecules in the hydrogels with anti-freezing agent (inorganic salts, organic solvents or ionic liquids), the freezing point could be decreased obviously [6–8]. Among them, organic solvents have attracted researchers' attention due to their low cost. They can inhibit ice crystal formation at subzero temperatures by forming hydrogen bonds with water molecules [9]. Li and co-workers synthesized a hydrogel with a broad temperature range from − 20 to 80 °C by using ethylene glycol as the anti-freezing agent [10]. Zheng and co-workers reported the application of an anti-freezing supercapacitor composed of polyvinyl alcohol (PVA), graphene, and dimethyl sulfoxide, which can work at an ultra-low temperature (−65 °C) [11]. Railanmaa and co-workers reported the performance of a supercapacitor with an electrolyte containing glycerol (Gly) at room temperature (RT) to − 30 °C [12]. Lu and co-workers introduced Gly and $CaCl_2$ to a PVA hydrogel, enhancing the freezing resistance of the organohydrogel [13]. Additionally, Wang and co-workers designed a Gly-water containing organohydrogel as a sensor, which has sensing stability in a range of − 20 to 60 °C [14].

Although organic solvents can inhibit ice crystals at low temperatures and prevent water evaporation at high

✉ Qing Xin
xinqing@hdu.edu.cn

1 Institute of Carbon Neutrality and New Energy, School of Electronics and Information, Hangzhou Dianzi University, Hangzhou 310018, People's Republic of China

temperatures, replacing water with organic solvents decreases the conductivity of organohydrogels [15]. Because organic solvents are non-conductive and can inhibit polymer ionization [16]. Conductivity is an essential parameter for electrolytes. To enable good ion transport, complexing metal into hydrogels seems to be an effective way. Zhang and co-workers incorporated polydopamine-Fe into the polyacrylamide network, enhancing the electrical conductivity of the hydrogel [17]. Bashir and co-workers introduced $MgTf_2$ into poly (N, N-dimethyl acrylamide) hydrogel electrolytes to improve the conductivity and stability of the hydrogels [18]. Xu and co-workers synthesized Kappa carrageenan interacting with K^+ to form an anion complex. Crosslinked with a poly(N-hydroxyethyl acrylamide) network, the obtained hydrogel exhibits multifunction in addition to good conductivity [19]. To our knowledge, there are not many reports about complexing metals with organic solvents. The work of Cevik et al. verified the ability of the supercapacitor with an anhydrous gel electrolyte of Mo-doped Gly-KOH to resist temperatures ranging from 0 to 100 °C [20].

To improve the low conductivity caused by the replacement of water with organic agents, we complexed transition metal Mo with Gly and embedded it into electrode and electrolyte bulk simultaneously. Due to its high capacitance, Mo oxide shows great potential as an electrode material for supercapacitors. The intermolecular chaining process between Gly and Mo makes the compound stable and improves ion transport. In addition to Gly-Mo, the supporting skeleton of organohydrogel electrolyte and the main active electrode material are PVA and polypyrrole (PPy). By growing the electrode in situ on the hydrogel electrolyte, we fabricate a flexible and anti-freezing multifunctional supercapacitor based on Gly-Mo. Owing to the introduction of Gly-Mo in both electrode and electrolyte, the interface resistance between the electrode and electrolyte is effectively decreased. The resultant supercapacitor shows outstanding energy storage performance even at the subzero temperature of − 40 °C and can work normally under short-term high temperatures. In addition, the in situ growth method makes the supercapacitor sustain punching and bending. These properties of the Gly-Mo-based supercapacitor pave the way for the development of energy storage devices with low temperature and damage resistance for wearable electronics.

Experimental section

Preparation of PVA/(Gly-Mo)$_X$ hydrogels

Firstly, Gly and $(NH_4)_2MoO_4$ solution in a mass ratio of 15:100 was stirred at 90 °C. After Gly-Mo ammonia gas was converted by ammonium, the obtained gel was Gly-Mo [20]. A 10 mL solution of H_2SO_4 (1 mol L^{-1}) was mixed with 2.5 g PVA and stirred at 90 °C. Gly-Mo was then added to the PVA polymer solution. After cooling, the above-mentioned solution was put into a mold. After three freezing-thawing cycles at − 20 °C and room temperature, we obtained fully physically crosslinked hydrogels. These hydrogels were called PVA/(Gly-Mo)$_X$, where X refers to the added volume of Gly-Mo (mL). Specifically, PVA/(Gly-Mo)$_3$, PVA/(Gly-Mo)$_5$, PVA/(Gly-Mo)$_8$, and PVA/(Gly-Mo)$_{11}$ were organohydrogels, and PVA/(Gly-Mo)$_0$ hydrogel was the control without Gly-Mo addition.

Preparation of supercapacitor

The PVA/(Gly-Mo)$_{8.7}$ organohydrogel was used as the electrolyte for the supercapacitor. The organohydrogel was dipped in a mixed pyrrole (412.5 μL) and a 15 mL H_2SO_4 (0.5 mol L^{-1}) solution. Polymerization was initiated by adding an ammonium persulfate (APS) mixed solution to the above-mentioned solution dropwise. The APS mixed solution contained 1.37 g APS, 3.6 mL Gly-Mo, and 15 mL H_2SO_4 solution (0.5 mol L^{-1}). After reacting for 6 h at 0–5 °C, washed, dried, and then cut off the edges, we obtained the flexible supercapacitor.

Characterization and electrochemical measurements

A Regulus8100 field emission scanning electron microscopy (FESEM, Hitachi, Japan) was adopted to observe the morphologies of PVA/(Gly-Mo)$_X$ hydrogels. A Nicolet iS5 Fourier transform infrared (FT-IR) spectra (Thermofisher Scientific, USA) was used to analyze the molecular structure of PVA/(Gly-Mo)$_X$ hydrogels. The electrochemical performance of the supercapacitor, which was cut into a size of 6 mm × 6 mm, was tested using a CHI660E electrochemical workstation (Chenhua, China), and the current collector was carbon paper. The specific areal capacitance (mF cm^{-2}) of the device was calculated using Eq. S1 (in Supporting Information) based on the galvanostatic charge-discharge (GCD) test. The vertical axis of the cyclic voltammetry (CV) curves represents the current density, which is obtained by dividing the current by the single-sided surface area of the supercapacitor.

Results and discussion

Properties of PVA/(Gly-Mo)$_X$ hydrogels

The flexibility of PVA/(Gly-Mo)$_X$ hydrogels at RT is compared with that after freezing at − 20 °C. The results shown in Fig. 1a display that PVA/(Gly-Mo)$_3$ and PVA/(Gly-Mo)$_5$ organohydrogels are frozen while PVA/(Gly-Mo)$_8$ and PVA/

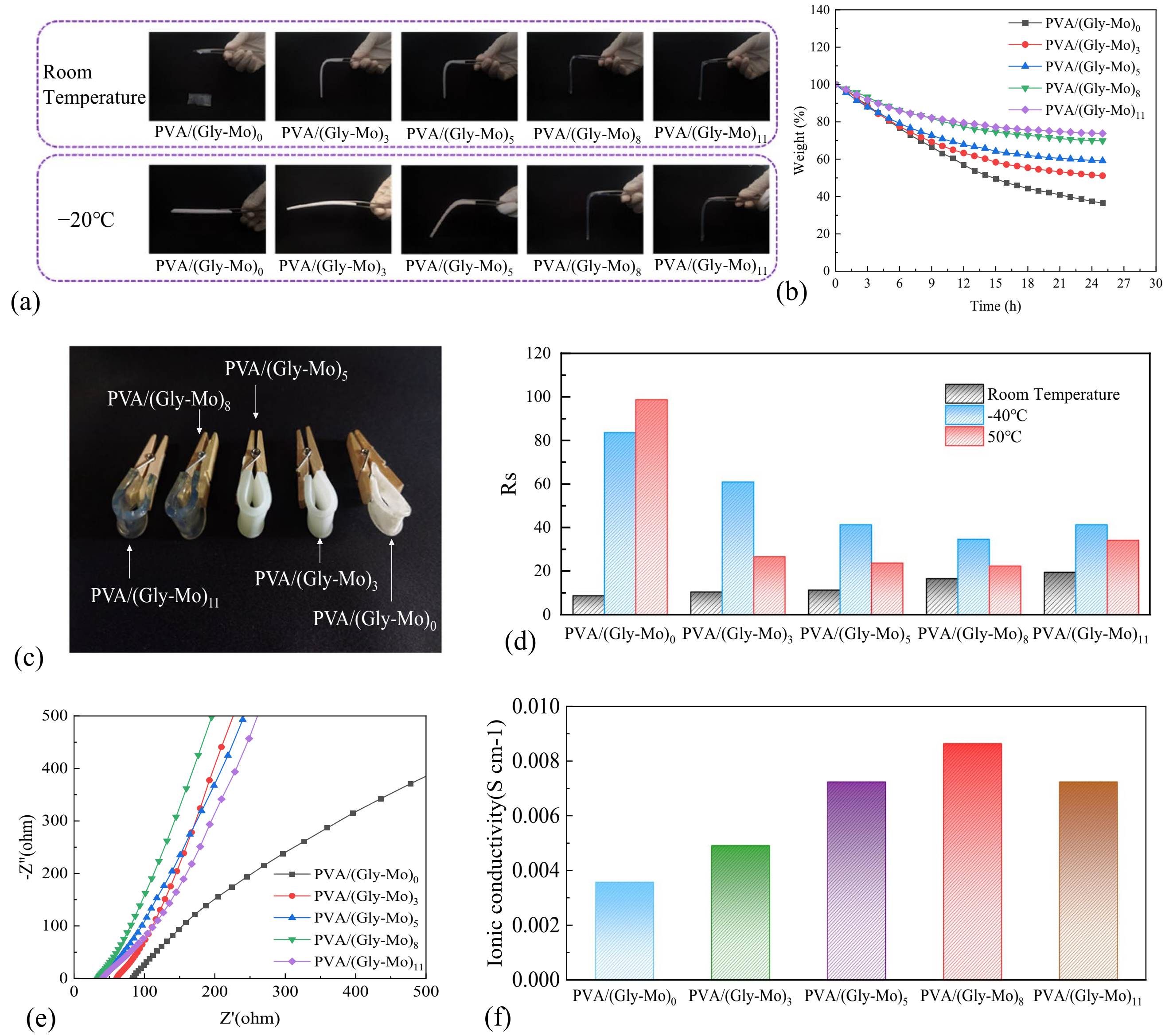

Fig. 1 **a** Flexibility of hydrogels at RT and − 20 °C; **b** the weight retention curves of hydrogels at 50 °C; **c** photographs of bending behavior of hydrogels at high temperature; **d** the Rs value of hydrogels at various temperature; **e** Nyquist plots of hydrogels at − 40 °C; **f** ionic conductivity of hydrogels at − 40 °C

$(Gly\text{-}Mo)_{11}$ organohydrogels are still flexible. It also shows that $PVA/(Gly\text{-}Mo)_0$ hydrogel can be easily broken even at room temperature, which verifies that the introduction of Gly-Mo enhanced the flexibility of the organohydrogels. The weight retention of $PVA/(Gly\text{-}Mo)_X$ hydrogels at 50 °C is shown in Fig. 1b. The weight of $PVA/(Gly\text{-}Mo)_X$ hydrogels decreases with the increase of time, owing to the loss of water. $PVA/(Gly\text{-}Mo)_0$ shows a rapid weight loss, and the increase of Gly-Mo content in organohydrogels slowed the trend. Figure 1c shows the photograph of the bending behavior of $PVA/(Gly\text{-}Mo)_X$ hydrogels at high temperature. At 50 °C for 24 h, the $PVA/(Gly\text{-}Mo)_0$ hydrogel looks like ice and has a slight crack after bending. The $PVA/(Gly\text{-}Mo)_3$ and $PVA/(Gly\text{-}Mo)_5$ organohydrogels with less Gly-Mo concentration turn white. In contrast, the $PVA/(Gly\text{-}Mo)_8$ and $PVA/(Gly\text{-}Mo)_{11}$ organohydrogels remain transparent and flexibility.

Equivalent series resistance (Rs) was determined by the high-frequency intercept on the real impedance axis in a Nyquist plot. The Rs of $PVA/(Gly\text{-}Mo)_X$ hydrogels at − 40 °C, RT, and 50 °C were compared, as shown in Fig. 1d. Though the Rs value of $PVA/(Gly\text{-}Mo)_0$ hydrogel is lower at RT, the Rs of $PVA/(Gly\text{-}Mo)_8$ performed better at high temperature and subfreezing temperature. From Figure S1, we can intuitively understand the influence of Gly-Mo on the conductivity of organohydrogels. Though the conductivity of PVA/(Gly-Mo)$_3$ organohydrogel visibly declines at − 20 °C, the conductivity of the others has no obvious change. It indicates that the Gly-Mo helps to maintain the high conductivity of the organohydrogels at subzero temperature.

To quantify the ionic conductivity at − 40 °C, the electrochemical impedance spectroscopy (EIS) test was conducted on PVA/(Gly-Mo)$_X$ at − 40 °C in the frequency range of 10^5–10^{-1} Hz (Fig. 1e). The values of ionic conductivity were calculated according to Eq. S2. Due to the anti-freezing performance of Gly-Mo, the organohydrogels exhibit better ionic conductivity at − 40 °C than PVA/(Gly-Mo)$_0$ hydrogel (Fig. 1f). Among them, PVA/(Gly-Mo)$_8$ displays the most outstanding ionic conductivity at subfreezing temperature. Nyquist plots of PVA/(Gly-Mo)$_8$ organohydrogel at different temperature can be seen in Figure S2. The conclusions above imply that a Gly-Mo-based organohydrogel has excellent ionic conductivity in extremely low temperature and high temperature, which is suitable for supercapacitors working at a wide temperature range.

The structure of the PVA/(Gly-Mo)$_X$ hydrogel is schematically illustrated in Fig. 2. PVA serves as the primary framework to provide satisfactory mechanical properties. Gly-Mo is embedded into the three-dimensional polymer network and responsible for the ionic conductivity and flexibility of the organohydrogels at subzero temperature. Due to the hydrogen bond, chain entanglements are formed between PVA and Gly-Mo. Gly can lower the freezing point, giving the organohydrogels anti-freezing property. Additionally, large amounts of Gly contribute to the full cross-linking of the PVA chains, forming supramolecular synergies [21].

The prepared organohydrogels have an increasing light transmittance compared to PVA/(Gly-Mo)$_0$ hydrogel, which is supported by UV-visible spectra (Figure S3). To quantify the effect of Gly-Mo content on the transparent properties of the hydrogels, Fig. 3a shows the light transmittance of PVA/(Gly-Mo)$_X$ at 400 and 550 nm. Furthermore, we can conclude that as the Gly-Mo concentration increases, the increase in transmittance becomes less pronounced. For instance, the amount of Gly-Mo was increased from 0 to 3 mL, and the light transmittance of the PVA/(Gly-Mo)$_3$ increased by 25.37% at 400 nm. While the light transmittance of the organohydrogel just increased by 3.14% at 400 nm as the amount of Gly-Mo further rises from 8 to 11 mL. The interaction between the hydroxyl groups in PVA and the hydrophilic groups in Gly-Mo forms hydrogen bonds, improving the microcrystalline region of PVA and thus increases the transmittance of the organohydrogels [22]. The transparency of organohydrogels enables them to transmit electrical signals without impeding optical signals, thus expanding their potential in the development of smart transparent windows for wearable electronics [23].

The interaction and structure formation between PVA and Gly-Mo was further identified by FT-IR spectra (Fig. 3b). The broad peaks around 3280 cm^{-1} are stretching vibration of −OH with slight shifting, caused by hydrogen bonding within crosslinking network [24]. The adsorption bands at ~ 2940 cm^{-1} and ~ 1420 cm^{-1} in the hydrogels corresponded to the C-H alkyl stretching vibration and -CH$_2$- of PVA, respectively [25, 26]. The intense adsorption bands at 1149–980 cm^{-1} belong to C-O stretching [20]. The peaks at 906 cm^{-1} and 854 cm^{-1} of PVA/(Gly-Mo)$_8$ organohydrogel are attributed to Mo-O-Mo bonds stretching vibration in Gly-Mo [27, 28]. The subtle shift of the adsorption peak is attributed to the complexation of Gly and Mo.

SEM images of PVA/(Gly-Mo)$_0$ hydrogel and PVA/(Gly-Mo)$_8$ organohydrogel exhibit the impact of Gly-Mo on the microstructure of organohydrogel. As shown in Fig. 3c, d, the PVA/(Gly-Mo)$_8$ organohydrogel presents more dense

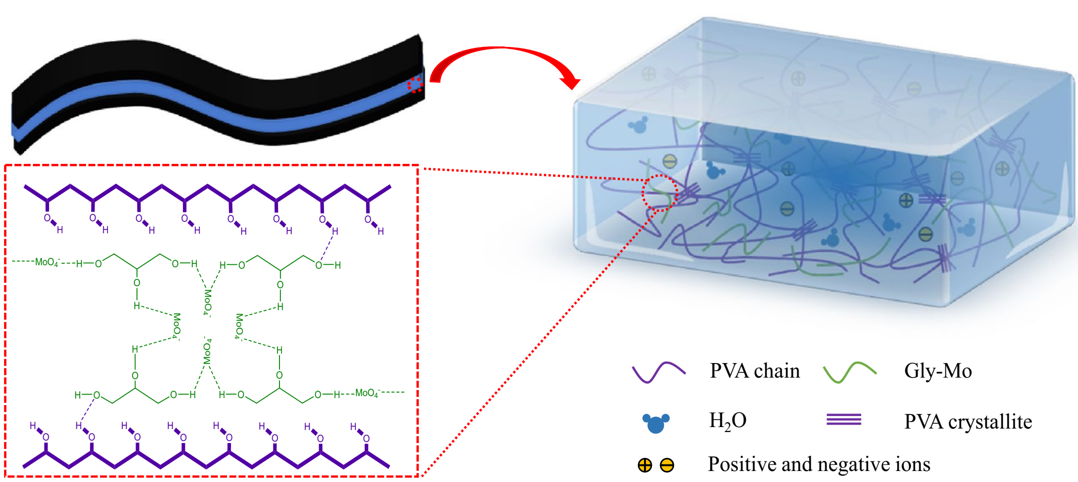

Fig. 2 Schematic illustration of the hydrogels

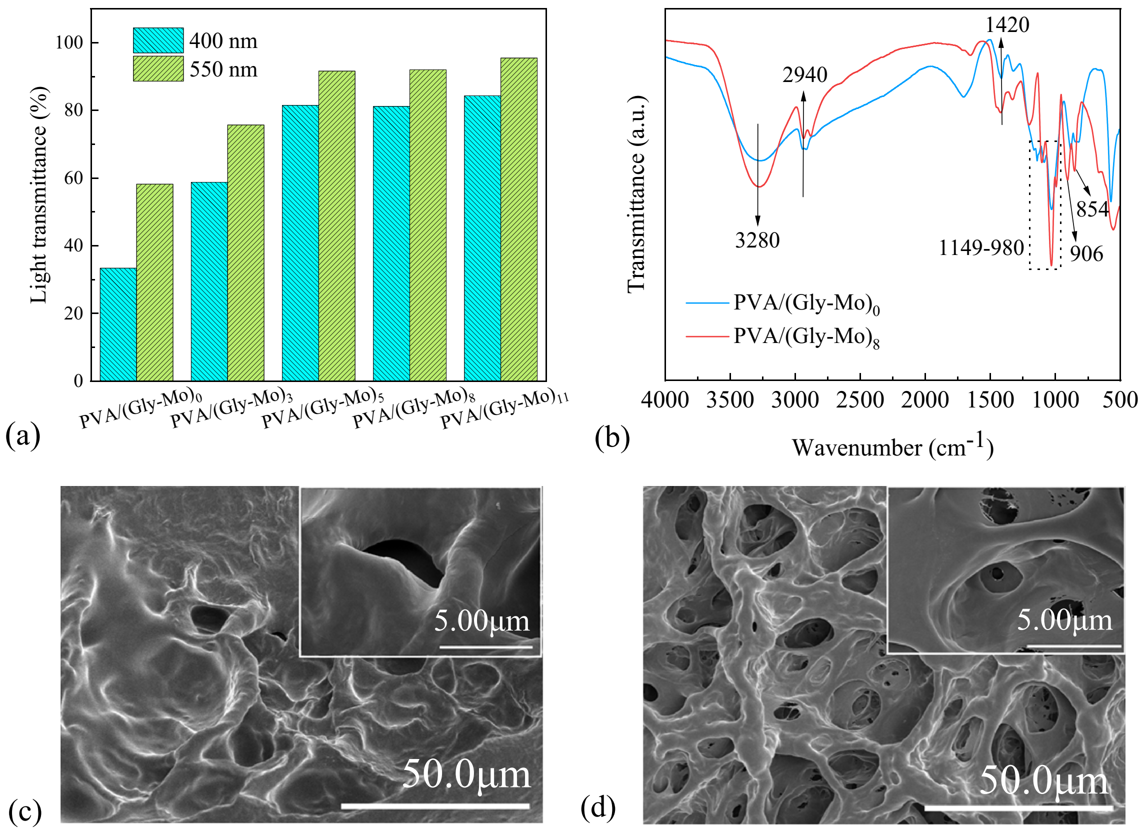

Fig. 3 **a** The effect of Gly-Mo concentration on the light transmittance of the organohydrogels; **b** FTIR spectra of PVA/(Gly-Mo)$_0$ and PVA/(Gly-Mo)$_8$; **c** SEM image of PVA/(Gly-Mo)$_0$; **d** SEM image of PVA/(Gly-Mo)$_8$

pores and hierarchical microstructure than the PVA/(Gly-Mo)$_0$ hydrogel. The Gly-Mo attributes to the high crosslinking network and 3D porous microstructure. Besides, the dense porous microstructure implies an enhanced porosity, more ion migration path, and increased conductivity of the organohydrogel [29]. To study the role of Gly-Mo on the mechanical property of the hydrogel, a compression test was conducted on PVA/(Gly-Mo)$_0$ and PVA/(Gly-Mo)$_8$ hydrogels. As revealed in Figure S4, the PVA/(Gly-Mo)$_8$ hydrogel can resist higher compressive stress during deformation, which can be attributed to its dense porous microstructure.

Electrochemical performances of the device at subzero temperature

To study the improved anti-freezing effect of PVA/(Gly-Mo)$_8$ organohydrogel, we fabricated a supercapacitor based on it, and the electrochemical properties of the device were measured at lower temperatures. From CV curves, we can see that although the enclosed area decreased at subzero temperatures compared with that at RT, the shape of the curves remains similar. It implies that the supercapacitor has electrochemical stability even at − 40 °C (Fig. 4a). The CV curve measured at − 40 °C shows a typical rectangular shape even at a high scan rate of 100 mV s^{-1} (Figure S5), demonstrating the good transfer rate of ions in the organohydrogel electrolyte and electrons in the electrode [30]. GCD curves of the device at different temperature are displayed in Fig. 4b. The specific capacitance of the device was 113.25 mF cm^{-2} at RT with a current density of 1 mA cm^{-2}. When measured at − 20 °C, the device delivered a specific capacitance of 90 mF cm^{-2}. As the temperature further dropped to − 40 °C, the device still exhibited 63.36% retention of specific capacitance at RT. Compared with other reported supercapacitor with PVA-based electrolyte hydrogels, the device with PVA/(Gly-Mo)$_8$ hydrogel exhibited a relatively higher specific capacitance retention rate at low temperatures (Table S1). To evaluate the durability of the device at low temperatures, we kept the device at − 20 °C for 24 h. According to GCD curves presented in Figure S6, the capacitance retention rate of the device remained 88.1% even after being stored at − 20 °C for 24 h.

The resistance behavior at various temperature revealed by Nyquist plots was matched well with the CV and GCD curves. As shown in Fig. 4c, the Rs increased from 8.6 to 23.8 Ω when the temperature reduced from RT to − 40 °C,

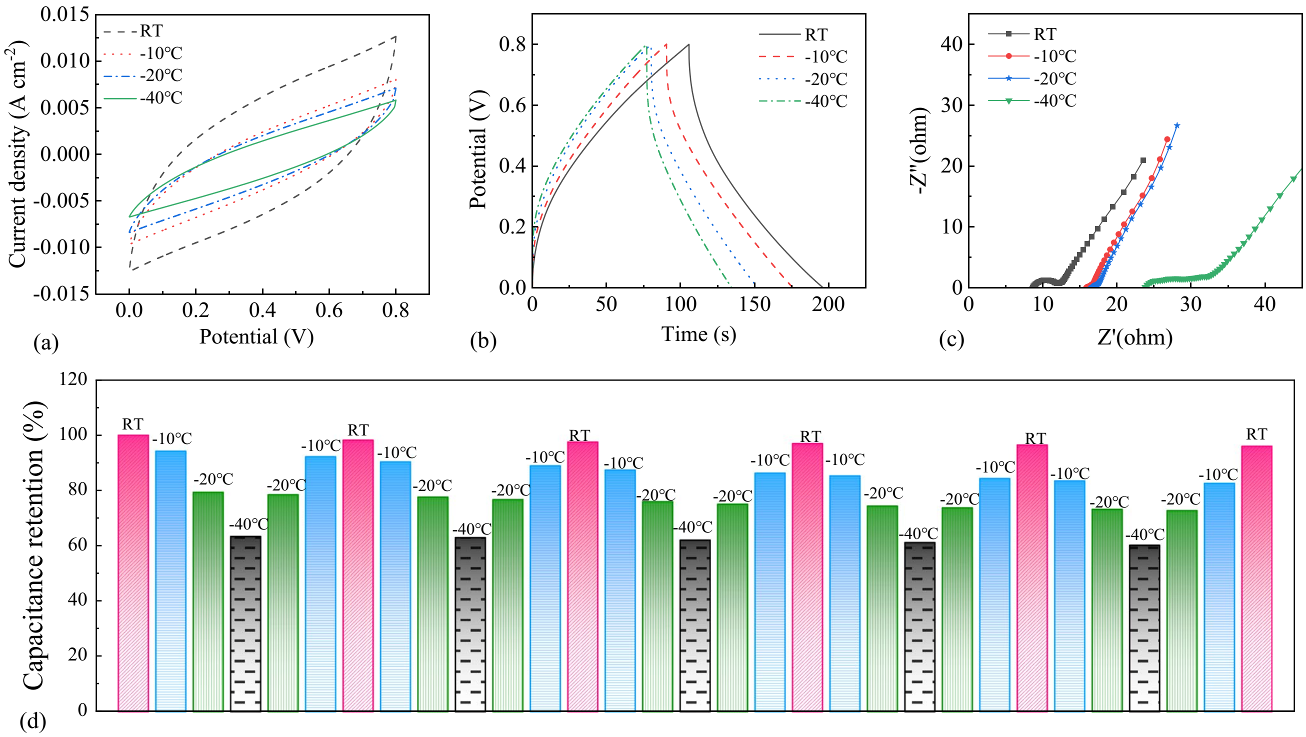

Fig. 4 Electrochemical performance device containing PVA/(Gly-Mo)$_8$ electrolyte at RT and varied subzero temperature: **a** CV curves at 100 mV s^{-1}; **b** GCD curves at 1 mA cm^{-2}; **c** Nyquist plots; **d** the cycles of reversible temperature changes

which was due to the slowing migration of electrolyte ions as temperature decreased [31]. Nevertheless, the Rs is still favorable even at − 40 °C, showing satisfactory low temperature tolerance of the device. Figure 4d exhibits five reversible temperature change cycles at RT, − 10 °C, − 20 °C, and − 40 °C. The specific capacitance of the supercapacitor with Gly-Mo organohydrogel electrolyte had almost no change, confirming its superior stable anti-freeze performance. Cycling charge-discharge tests at low temperatures was also conducted, as shown in Figure S7. After 50 charge-discharge cycles at − 10 °C, the specific capacitance retention rate of the supercapacitor was 64.2%. Even after 50 charge-discharge cycles at − 40 °C, the specific capacitance retention rate of the device remained at 37%, indicating that it can still work properly.

Electrochemical performances of the device with punching, bending, and drying

Resistance to damage, flexibility and short-term high temperature are crucial for wearable electronic energy storage devices. We punched holes in the supercapacitor to evaluate its ability to withstand sudden puncture. The electrochemical behavior of the device with 300, 600, and 900 holes cm^{-2} is exhibited in Fig. 5a–c. CV curves show that the device remains stable even when the number of holes is as high as 900 holes cm^{-2}. The GCD curves further confirm these holes have no negative effect on the energy storage performance of the device. In fact, with hole number of 300 holes cm^{-2}, the specific capacitance reached 140.75 mF cm^{-2} at 1 mA cm^{-2}, which was nearly 124.28% retention of the initial value. This phenomenon may be attributed to the easy penetration of conductive ions in the electrolyte into the active substance through the holes [32]. The result shown in Nyquist plots of devices with holes was consistent with that of GCD curves. The devices with through-holes display a lower Rs value than the original one. It is worth noting that when the hole number further increased to 600 or 900 holes cm^{-2}, the electrochemical behavior showed a slightly declining trend.

We fabricated a device with a length of 24 mm and tested its bending performance. The electrochemical performance of the supercapacitor after bending can be seen in Fig. 5d–f. After 400 times bending, the integral area of CV curve is reduced, but the shape of the curve keeps similar. It means the good adhesion between electrodes and electrolyte even after hundreds of bending [4]. From GCD analysis, the specific capacitance remained 77.13 mF cm^{-2} (approximately 68.1% retention of the initial one) after being bent to 90° for 400 times, verifying the outstanding mechanical properties of the device. From Nyquist plots, the bulk resistance of the device increased with increasing bending time. The Rs value

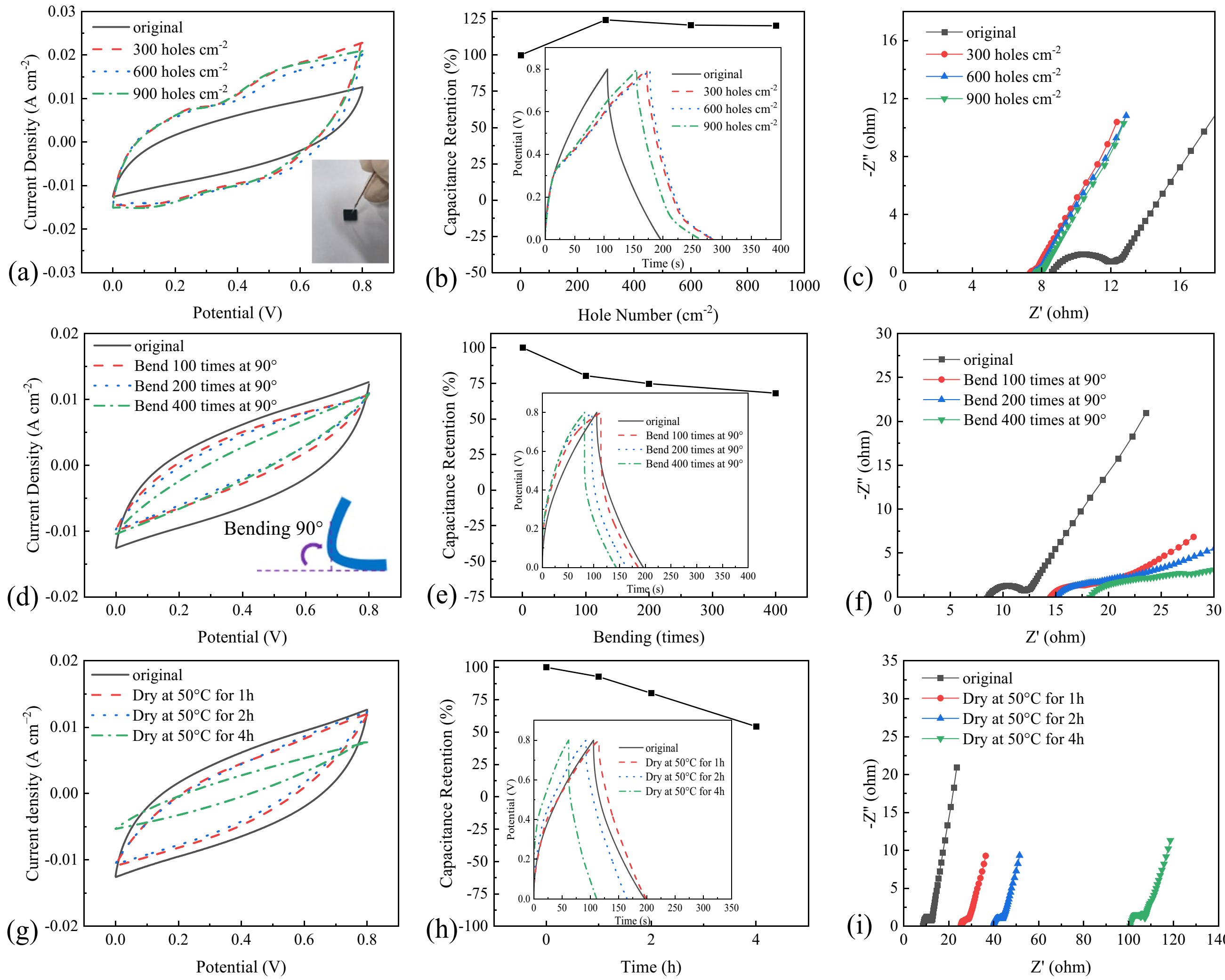

Fig. 5 Electrochemical behavior of the device containing PVA/(Gly-Mo)$_8$ electrolyte after (**a**–**c**) punching, **d**–**f** bending, and (**g**–**i**) drying at 50 °C

was 18.45 Ω after 400 bending times, which was acceptable for a flexible supercapacitor. It is worth mentioning that, as shown in Figure S8, under low-temperature conditions, the supercapacitor also maintains similar bending performance as it does at room temperature.

Being able to function at high temperatures, such as in a hot desert, is an indispensable requirement for a wearable electronic energy storage device. As shown in Fig. 5g–i, high temperature has an obviously negative effect on the energy storage of the device. Though the shape of the CV curve was kept well, the specific capacitance from GCD test was reduced with the increased drying time. The capacitance retention was 54.3% when the device withstands 50 °C for 4 h. The Rs value was ~ 40 Ω for 2 h at 50 °C but dramatically increased to ~ 100 Ω when exposed to the high temperature for 4 h. The discrepancy of the thermal expansion coefficient between electrolyte and electrode materials weakens the interfacial interactions between them, thus affecting the device performance [33]. These phenomena verify that supercapacitor containing the PVA/(Gly-Mo)$_8$ organohydrogel electrolyte possesses outstanding freeze resistance and can be used under temporary high-temperature condition. Hydrogen bonds between Gly and water molecules in the organohydrogel take place of those among water molecules, thus preventing ice lattice formation as well as water evaporation [14].

Conclusion

In summary, we have designed a supercapacitor whose electrode and electrolyte both contain Gly-Mo complex. The role of Gly-Mo in the flexibility and conductivity of organohydrogels was discussed. The organohydrogel PVA/(Gly-Mo)$_8$

showed good flexibility and conductivity at a wide temperature range of − 40 to 50 °C. Replacing water molecules in the hydrogels with Gly-Mo improved the supercapacitor's low-temperature tolerance, with 63.36% retention of specific capacitance as the temperature dropped to − 40 °C. In addition, punching on the device had no obvious negative influence on its electrochemical performance. After bent to 90° for 400 times, the specific capacitance retention was kept 68.1%. The results verify that the design of the supercapacitor effectively improves the conductivity and low temperature tolerance.

Supplementary Information The online version contains supplementary material available at https://doi.org/10.1007/s11581-023-05140-6.

Author contribution Qing Xin: investigation, writing—original draft, and funding acquisition. Xiaojie Chu: methodology, formal analysis, and investigation. Guoqing Yang: supervision. Shangqing Liang: conceptualization. Jun Lin: project administration.

Funding This work was supported by the Zhejiang Provincial Natural Science Foundation of China (grant no. LY17B060012).

Data availability Not applicable.

Declarations

Ethical approval Not applicable.

Competing interests The authors declare no competing interests.

References

1. Xu T, Yang DZ, Zhang SY, Zhao TY, Zhang M, Yu ZZ (2021) Antifreezing and stretchable all-gel-state supercapacitor with enhanced capacitances established by graphene/PEDOT-polyvinyl alcohol hydrogel fibers with dual networks. Carbon 171:201–210. https://doi.org/10.1016/j.carbon.2020.08.071
2. Hu O, Chen G, Gu J, Lu J, Zhang J, Zhang X, Hou L, Jiang X (2020) A facile preparation method for anti-freezing, tough, transparent, conductive and thermoplastic poly(vinyl alcohol)/sodium alginate/glycerol organohydrogel electrolyte. Int J Biol Macromol 164:2512–2523. https://doi.org/10.1016/j.ijbiomac.2020.08.115
3. Cheng T, Zhang YZ, Wang S, Chen YL, Gao SY, Wang F, Lai WY, Huang W (2021) Conductive hydrogel-based electrodes and electrolytes for stretchable and self-healable supercapacitors. Adv Funct Mater 31:2101303. https://doi.org/10.1002/adfm.202101303
4. Hu Q, Cui S, Sun K, Shi X, Zhang M, Peng H, Ma G (2022) An antifreezing and thermally stable hydrogel electrolyte for high-performance all-in-one flexible supercapacitor. J Energy Storage 50:104231. https://doi.org/10.1016/j.est.2022.104231
5. Lu N, Na R, Li L, Zhang C, Chen Z, Zhang S, Luan J, Wang G (2020) Rational design of antifreezing organohydrogel electrolytes for flexible supercapacitors. ACS Appl Energy Mater 3:1944–1951. https://doi.org/10.1021/acsaem.9b02379
6. Qin C, Lu A (2021) Flexible, anti-freezing self-charging power system composed of cellulose based supercapacitor and triboelectric nanogenerator. Carbohydr Polym 274:118667. https://doi.org/10.1016/j.carbpol.2021.118667
7. Huang M, Shi H, Wei N, Luo C, Luo F (2021) An ultra-strong, ultra-stiff and anti-freezing hydrogel based on poly (vinyl alcohol). Mater Lett 300:130172. https://doi.org/10.1016/j.matlet.2021.130172
8. Hu Q, Shi X, Sun K, Cui S, Hamouda HA, Zhang W, Peng H, Ma G (2022) A super-stretchable and thermally stable hydrogel electrolyte for high performance supercapacitor with wide operation temperature. J Alloys Compd 909:164646. https://doi.org/10.1016/j.jallcom.2022.164646
9. Hu O, Lu J, Chen G, Chen K, Gu J, Weng S, Hou L, Zhang X, Jiang X (2021) An antifreezing, tough, rehydratable, and thermoplastic poly(vinyl alcohol)/sodium alginate/poly(ethylene glycol) organohydrogel electrolyte for flexible supercapacitors. ACS Sustain Chem Eng 9:9833–9845. https://doi.org/10.1021/acssuschemeng.1c02464
10. Li X, Lou D, Wang H, Sun X, Li J, Liu YN (2020) Flexible supercapacitor based on organohydrogel electrolyte with long-term anti-freezing and anti-drying property. Adv Funct Mater 30:2007291. https://doi.org/10.1002/adfm.202007291
11. Zheng H, Guan R, Liu Q, Ou K, Li D, Fang J, Fu Q, Sun Y (2022) A flexible supercapacitor with high capacitance retention at an ultra-low temperature of-65.0 degrees C. Electrochim Acta 424:140644. https://doi.org/10.1016/j.electacta.2022.140644
12. Railanmaa A, Lehtimaki S, Keskinen J, Lupo D (2019) Non-toxic printed supercapacitors operating in sub-zero conditions. Sci Rep 9:14059. https://doi.org/10.1038/s41598-019-50570-w
13. Lu J, Gu J, Hu O, Fu Y, Ye D, Zhang X, Zheng Y, Hou L, Liu H, Jiang X (2021) Highly tough, freezing-tolerant, healable and thermoplastic starch/poly(vinyl alcohol) organohydrogels for flexible electronic devices. J Mater Chem A 9:18406–18420. https://doi.org/10.1039/d1ta04336f
14. Wang J, Dai T, Zhou Y, Mohamed A, Yuan G, Jia H (2022) Adhesive and high-sensitivity modified Ti_3C_2Tx (MXene)-based organohydrogels with wide work temperature range for wearable sensors. J Colloid Interface Sci 613:94–102. https://doi.org/10.1016/j.jcis.2022.01.021
15. Gu J, Huang J, Chen G, Hou L, Zhang J, Zhang X, Yang X, Guan L, Jiang X, Liu H (2020) Multifunctional poly(vinyl alcohol) nanocomposite organohydrogel for flexible strain and temperature sensor. ACS Appl Mater Interfaces 12:40815–40827. https://doi.org/10.1021/acsami.0c12176
16. Chen J, Yu Q, Shi D, Yang Z, Dong K, Kaneko D, Dong W, Chen M (2021) Tough and antifreezing organohydrogel electrolyte for flexible supercapacitors with wide temperature stability. ACS Appl Energy Mater 4:9353–9361. https://doi.org/10.1021/acsaem.1c01556
17. Zhang X, Peng Y, Wang X, Ran R (2021) Melanin-inspired conductive hydrogel sensors with ultrahigh stretchable, self-healing, and photothermal capacities. ACS Appl Polym Mater 3:1899–1911. https://doi.org/10.1021/acsapm.0c01430
18. Bashir S, Hina M, Iqbal J, Jafer R, Ramesh S, Ramesh K (2022) Self-healable poly (N, N-dimethylacrylamide)/poly (3,4-ethylenedioxythiophene) polystyrene sulfonate composite hydrogel electrolytes for aqueous supercapacitors. J Energy Storage 45:103760. https://doi.org/10.1016/j.est.2021.103760
19. Xu J, Guo Z, Chen Y, Luo Y, Xie S, Zhang Y, Tan H, Xu L, Zheng J (2021) Tough, adhesive, self-healing, fully physical crosslinked kappa-CG-K^+/pHEAA double-network ionic conductive hydrogels for wearable sensors. Polymer 236:124321. https://doi.org/10.1016/j.polymer.2021.124321
20. Cevik E, Gunday ST, Bozkurt A, Amine R, Amine K (2020) Bio-inspired redox mediated electrolyte for high performance flexible supercapacitor applications over broad temperature domain. J Power Sources 474:228544. https://doi.org/10.1016/j.jpowsour.2020.228544

21. Zhu K, Han X, Ye S, Cui P, Dou L, Ma W, Tao X, Wei X, Heng S (2022) Flexible all-in-one supercapacitors enabled by self-healing and anti-freezing polymer hydrogel electrolyte. J Energy Storage 53:105096. https://doi.org/10.1016/j.est.2022.105096
22. Pan Y, Ding J, Chen Y, Shen Q (2016) Study on mechanical and optical properties of poly(vinyl alcohol) hydrogel used as soft contact lens. Mater Technol (N Y N Y) 31:266–273. https://doi.org/10.1179/1753555715Y.0000000052
23. Qin C, Lu A (2021) Flexible, anti-freezing self-charging power system composed of cellulose based supercapacitor and triboelectric nanogenerator. Carbohyd Polym 274:118667. https://doi.org/10.1016/j.carbpol.2021.118667
24. Wu S, Tang L, Xu Y, Yao J, Tang G, Dai B, Wang W, Tang J, Gong L (2022) A self-powered flexible sensing system based on a super-tough, high ionic conductivity supercapacitor and a rapid self-recovering fully physically crosslinked double network hydrogel. J Mater Chem C 10:3027–3035. https://doi.org/10.1039/d1tc04514h
25. Zheng H, Lin N, He Y, Zuo B (2021) Self-healing, self-adhesive silk fibroin conductive hydrogel as a flexible strain sensor. ACS Appl Mater Interfaces 13:40013–40031. https://doi.org/10.1021/acsami.1c08395
26. Li G, Zhang X, Sang M, Wang X, Zuo D, Xu J, Zhang H (2021) A supramolecular hydrogel electrolyte for high-performance supercapacitors. J Energy Storage 33:101931. https://doi.org/10.1016/j.est.2020.101931
27. Ghosh K, Yue CY (2018) Development of 3D MoO_3/graphene aerogel and sandwich-type polyaniline decorated porous MnO_2–graphene hybrid film based high performance all-solid-state asymmetric supercapacitors. Electrochim Acta 276:47–63. https://doi.org/10.1016/j.electacta.2018.04.162
28. Kamalam MBR, Inbanathan SSR, Sethuraman K (2018) Enhanced photo catalytic activity of graphene oxide /MoO_3 nanocomposites in the degradation of Victoria Blue Dye under visible light irradiation. Appl Surf Sci 449:685–696. https://doi.org/10.1016/j.apsusc.2017.12.099
29. Huang J, Peng S, Gu J, Chen G, Gao J, Zhang J, Hou L, Yang X, Jiang X, Guan L (2020) Self-powered integrated system of strain sensor and flexible all solid-state supercapacitor by using high performance ionic organohydrogel. Mater Horizons 7:2085–2096. https://doi.org/10.1039/d0mh00100g
30. Liu JH, Khanam Z, Ahmed S, Wang HT, Wang T, Song SH (2021) A study of low-temperature solid-state supercapacitors based on Al-ion conducting polymer electrolyte and graphene electrodes. J Power Sources 488:229461. https://doi.org/10.1016/j.jpowsour.2021.229461
31. Feng EK, Li JJ, Zheng GC, Yan Z, Li X, Gao W, Ma XX, Yang ZM (2021) Long-term anti-freezing active organohydrogel based superior flexible supercapacitor and strain sensor. ACS Sustain Chem Eng 9:7267–7276. https://doi.org/10.1021/acssuschemeng.1c01209
32. Zou Y, Chen C, Sun Y, Gan S, Dong L, Zhao J, Rong J (2021) Flexible, all-hydrogel supercapacitor with self-healing ability. Chem Eng J 418:128616. https://doi.org/10.1016/j.cej.2021.128616
33. Hou XL, Zhang Q, Wang LY, Gao GH, Lu W (2021) Low-temperature-resistant flexible solid supercapacitors based on organohydrogel electrolytes and microvoid-incorporated reduced graphene oxide electrodes. ACS Appl Mater Interfaces 13:12432–12441. https://doi.org/10.1021/acsami.0c18741

Publisher's note Springer Nature remains neutral with regard to jurisdictional claims in published maps and institutional affiliations.